

Momentum injection in tokamak plasmas and transitions to reduced transport

F. I. Parra,^{1,2,*} M. Barnes,^{1,3,2} E. G. Highcock,^{1,2} A. A. Schekochihin,^{1,2} and S. C. Cowley^{3,2}

¹Rudolf Peierls Centre for Theoretical Physics, University of Oxford, Oxford OX1 3NP, UK

²Isaac Newton Institute for Mathematical Sciences, Cambridge CB3 0EH, UK

³Euratom/CCFE Fusion Association, Culham Science Centre, Abingdon OX14 3DB, UK

(Dated: October 31, 2018)

The effect of momentum injection on the temperature gradient in tokamak plasmas is studied. A plausible scenario for transitions to reduced transport regimes is proposed. The transition happens when there is sufficient momentum input so that the velocity shear can suppress or reduce the turbulence. However, it is possible to drive too much velocity shear and rekindle the turbulent transport. The optimal level of momentum injection is determined. The reduction in transport is maximized in the regions of low or zero magnetic shear.

PACS numbers: 52.25.Fi, 52.30.-q, 52.55.Fa

Introduction. In this Letter, we study the effect of velocity shear on turbulent transport in tokamaks to answer two questions: (a) what is the optimal momentum input that minimizes radial energy transport? and (b) under what conditions do abrupt transitions to reduced transport regimes occur? Experimentally, tokamak plasmas can develop regions of reduced transport where the temperature gradient is much higher than the typical value for the same energy input [1], leading to more stored energy and better performance at less cost. In large tokamaks, these Internal Transport Barriers (ITBs) are found in regimes with low magnetic shear and with a net momentum input by neutral beams [2, 3]. In previous work, flow shear [4–7] and the Shafranov shift [8] have been proposed as causes for the transition to reduced transport. Here we highlight the physical influence of the velocity shear and momentum input. Employing basic properties of the turbulent transport deduced from new numerical results [6, 7] we show that there is an optimal level of momentum input, and prove that abrupt transitions to reduced transport are possible because the steady state transport equations have several solutions, allowing for bifurcations. We also obtain the conditions under which transitions can occur.

State of numerical evidence. Refs. [6, 7] studied numerically the effect of flow shear on the turbulent ion

radial energy flux Q_t with finite [6] and zero [7] magnetic shear. In Fig. 1, we sketch the dependence of Q_t on the dimensionless parameters $\kappa = R/L_T$ and $\gamma_E = (B_P/B_T)(R^2/v_{ti})|\partial\omega/\partial r|$, where $L_T = |d(\ln T_i)/dr|^{-1}$ is the scale of variation of the ion temperature, ω is the rotation rate, v_{ti} is the ion thermal speed, r and R are the minor and major radius, and B_T and B_P are the toroidal and poloidal magnetic field. The energy flux is normalized by the gyroBohm value $Q_{gB} = (\rho_i/R)^2 p_i v_{ti}$, with p_i and ρ_i the ion pressure and gyroradius. The curves in Fig. 1 are generated by a simple analytic model chosen to approximate the zero magnetic shear results of [7]. For every κ , there is a minimum Q_t , and for sufficiently small κ , this minimum is zero. For large γ_E , the parallel velocity gradient drives an instability that rekindles the turbulence [9, 10]. The dependence of Q_t on κ and γ_E is qualitatively similar for finite magnetic shear [6], but quantitatively there is a considerable difference: with zero magnetic shear, the minima in Q_t are much smaller for the same κ , and the region of γ_E for which the turbulence is suppressed is wider.

The turbulent flux of toroidal angular momentum Π_t was also calculated in [6, 7]. It is also normalized by the gyroBohm value $\Pi_{gB} = (\rho_i/R)^2 R p_i$. The dependence of Π_t on κ and γ_E has a remarkable property: defining the normalized turbulent diffusivities as $\chi_t = Q_t/\kappa$ and $\nu_t = \Pi_t/[(B_T/B_P)\gamma_E]$, the turbulent Prandtl number $Pr_t = \nu_t/\chi_t$ was found to be approximately independent of κ and γ_E and of order unity [16].

Graphical analysis. We analyze a plasma heated by neutral beams. Consider a flux surface that contains the volume inside which the energy and momentum are deposited. The ratio of the injected momentum and energy fluxes is $\Pi_b/Q_b \sim C v_{ti}/V_b$, where V_b is the beam velocity, C is a geometrical constant dependent on the angle of the beams and Π_b and Q_b are normalized by the gyroBohm values. Thus, Π_b/Q_b is a constant that only depends on the characteristics of the beam. In experiments, Π_b/Q_b is usually of the order of 0.1 [11].

To determine κ and γ_E , we need to solve the equa-

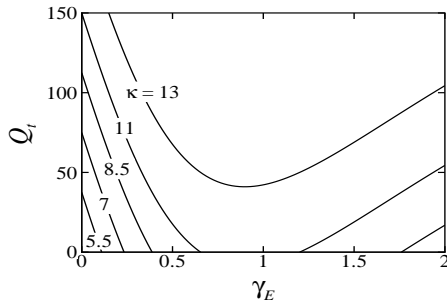


FIG. 1: Schematic dependence of the turbulent energy flux Q_t on the velocity shear γ_E and the temperature gradient κ .

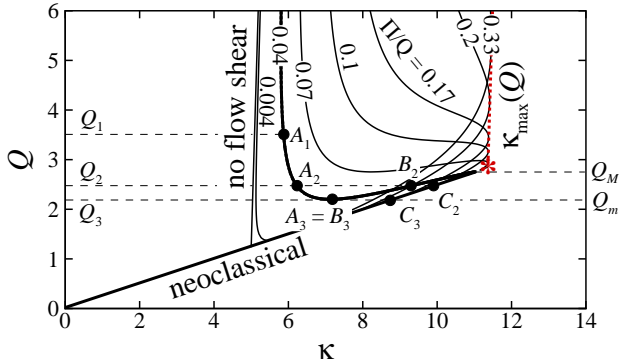


FIG. 2: Energy flux Q vs. temperature gradient κ for a constant ratio Π/Q of momentum and energy input.

tions $Q = Q_t + Q_n = Q_b$ and $\Pi = \Pi_t + \Pi_n = \Pi_b$ [17], where $Q_n = \chi_n \kappa$ and $\Pi_n = \nu_n (B_T/B_P) \gamma_E$ are the collisional *neoclassical* energy and momentum fluxes [12]. The dimensionless diffusivities χ_n and ν_n are proportional to the ion-ion collision frequency and depend on the magnetic field geometry. Importantly, the neoclassical Prandtl number $Pr_n = \nu_n/\chi_n \sim 0.1$ is smaller than the turbulent Prandtl number $Pr_t \sim 1$ [12].

To describe the solutions to $Q = Q_b$ and $\Pi = \Pi_b$, we plot the curves of constant Π/Q in a (κ, Q) graph, as given in Fig. 2 [18]. The beam characteristics determine the curve of constant Π/Q . Then, given Q , the temperature gradient κ is easy to read off the graph.

To understand Fig. 2, it is convenient to consider the (γ_E, κ) parameter space and search for points of intersection of curves of constant Q and Π/Q . From the general shape of the constant κ curves in Fig. 1, we infer the contours of constant Q in the (γ_E, κ) plane, shown in Fig. 3(a). The transport is purely neoclassical for κ below the critical value $\kappa_c(\gamma_E)$ (this corresponds to the points in Fig. 1 where Q_t vanishes; it is *not* the linear stability boundary [19]). At $\kappa < \kappa_c$, the constant Q curves are horizontal because Q_n is independent of γ_E . At $\kappa > \kappa_c$, since neoclassical transport is usually much smaller than turbulent transport, the constant Q curves are approximately the constant Q_t curves. We stress that $\kappa_c(\gamma_E)$ is the curve of $Q_t = 0$, but it is *not* a curve of constant $Q = Q_t + Q_n$. In Fig. 3(a), we have exaggerated the difference.

The curves of constant Π/Q are also shown in Fig. 3(a). For $\kappa < \kappa_c$, the transport is neoclassical, and for $\kappa \gg \kappa_c$, turbulence dominates. Therefore

$$\kappa = (\Pi/Q)^{-1} Pr_n (B_T/B_P) \gamma_E \quad \text{for } \kappa < \kappa_c, \quad (1)$$

$$\kappa = (\Pi/Q)^{-1} Pr_t (B_T/B_P) \gamma_E \quad \text{for } \kappa \gg \kappa_c. \quad (2)$$

In both regimes, the curves of constant Π/Q are straight lines passing through the origin. Since $Pr_t > Pr_n$, these lines are steeper in the turbulent than in the neoclassical regime. To transit from the former to the latter, the

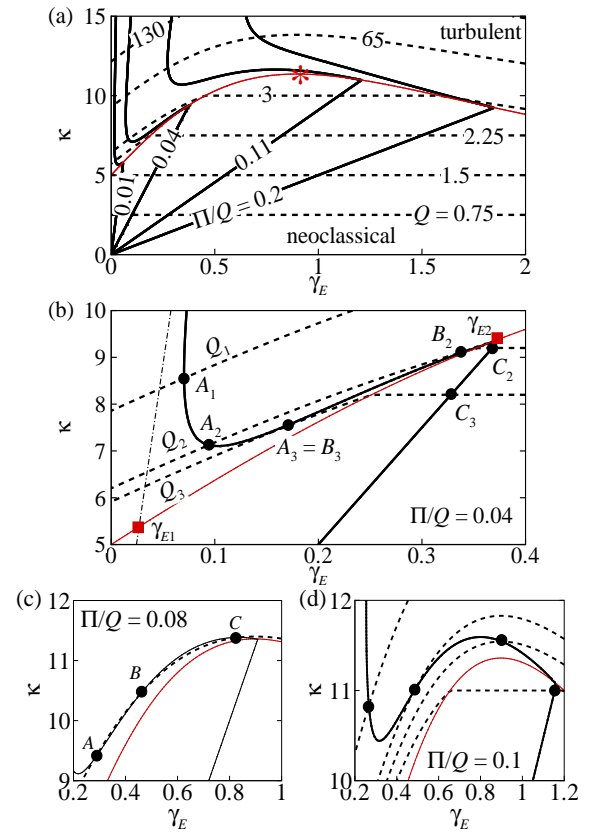


FIG. 3: (a) Curves of constant Q (dashed lines) and constant Π/Q (solid lines). The thin red line is the critical temperature gradient κ_c below which there is no turbulence. (b) Sketch of the intersection between a curve of given Π/Q and curves of constant Q with $Q_1 > Q_2 > Q_3$. The black dash-dot line is Eq. (2). (c), (d) Similar sketches for higher Π/Q .

curves of constant Π/Q must approximately follow the curve $\kappa_c(\gamma_E)$ because neoclassical and turbulent transport are comparable in its vicinity. In Fig. 3(a), the transition from Eq. (1) to Eq. (2) is shown in detail by exaggerating the difference between the constant Π/Q curve and $\kappa_c(\gamma_E)$. This piece of the curve of constant Π/Q is crucial for bifurcations.

Fig. 2 was produced using Fig. 3(a). The intersections of constant Q and constant Π/Q curves for $\kappa \gg \kappa_c$ correspond to the high Q section of the curves in Fig. 2, and the intersections for $\kappa < \kappa_c$ form the neoclassical straight line. The region in between, where for each value of Q and Π we can find several values of κ , is examined in the (γ_E, κ) space below in the section on bifurcations.

Optimal momentum injection. In Fig. 2, it is clear that to maximize κ , we need to operate on the red dashed line $\kappa_{\max}(Q)$ that corresponds to the the maxima in κ at constant Q in Fig. 3(a). However, once there, any increase in κ achieved by increasing the energy input Q is small because turbulent transport is very stiff. Therefore, the optimal operation is at the maximum critical tempera-

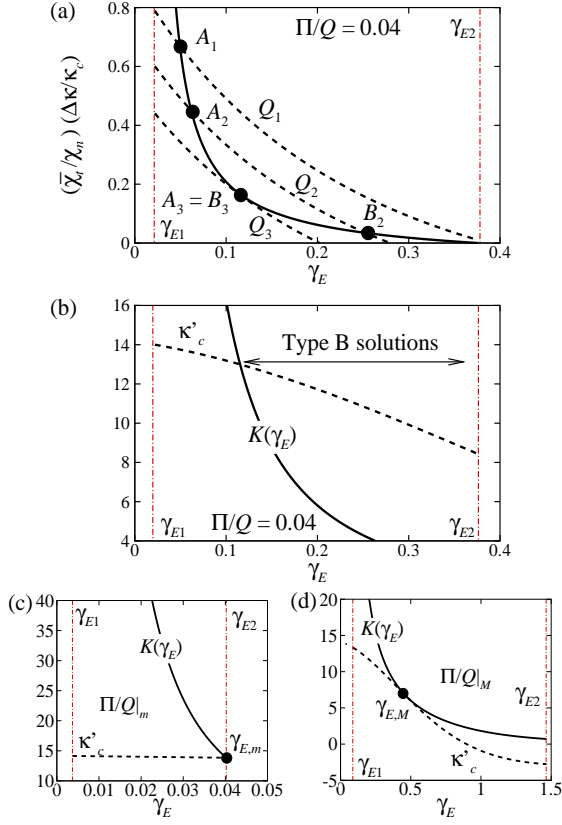


FIG. 4: (a) Asymptotic approximation to the curves of constant Q (dashed lines) and constant Π/Q (solid lines) in the transition region between neoclassical and turbulent regimes. (b) Graphical representation of condition (5) for type B solutions to exist. (c), (d) The cases in which type B solutions no longer exist for small and large Π/Q .

ture gradient, $\kappa_{c,\max} = \kappa_c(\gamma_{E,\max})$, given in Fig. 2 and Fig. 3(a) as a red star. As a result, the optimal temperature gradient is $\kappa_{c,\max}$, the optimal momentum input is $\Pi/Q = (B_T/B_P)Pr_n(\gamma_{E,\max}/\kappa_{c,\max})$, and the optimal energy flux is $Q = \chi_n\kappa_{c,\max}$.

Conditions for bifurcations. Transitions can happen only when there are several values of κ and γ_E for given values of Q and Π . The curves of constant Q and constant Π/Q can intersect in multiple points, as exemplified by the thicker line in Fig. 2. Fig. 3(b) is a sketch of the curves in the (γ_E, κ) plane that correspond to this case. For $Q = Q_1$, turbulence dominates and there is only one solution, A_1 . If we decrease the energy input to Q_2 , there are three solutions A_2, B_2 and C_2 , where C_2 is neoclassical. A jump from A_2 to C_2 reduces the transport and increases the temperature gradient. If we continue decreasing Q to Q_3 , the constant Q and Π/Q curves become tangent and there are two solutions. For $Q < Q_3$, there is only one solution, which is neoclassical.

Increasing Π/Q above the value in Fig. 3(b) gives the curves in Fig. 3(c). The solution C with the largest κ is

not purely neoclassical because the large momentum input causes a large parallel velocity gradient, which drives turbulence [6, 7, 9, 10]. At even larger Π/Q , the situation is as in Fig. 3(d), where there is only one solution for each Q and bifurcations are not possible. It is easy to see how these cases are reflected in the large Π/Q curves of Fig. 2. We now discuss the conditions for several solutions to exist.

Compare Figs. 3(b) and 3(d). The existence of several solutions is determined by the slope of the piece of the curve of constant Π/Q that transits between the neoclassical and turbulent regimes. We study that region to prove that to have several solutions and hence transitions, Π/Q and Q must be within a domain determined by the shape of the curve $\kappa_c(\gamma_E)$. Near this critical curve, $Q_t \simeq \bar{\chi}_t(\gamma_E)[\kappa - \kappa_c(\gamma_E)]$, where $\bar{\chi}_t = \kappa_c(\partial\chi_t/\partial\kappa)|_{\kappa=\kappa_c}$ and $\Delta\kappa = \kappa - \kappa_c \ll \kappa_c$. We also assume that Pr_t remains approximately constant even for $\kappa \simeq \kappa_c$. Then, expanding in $\chi_n/\bar{\chi}_t \ll 1$ and ordering $Pr_t \sim Pr_n \sim 1$, we find the curves of constant Q and Π/Q to be

$$\Delta\kappa_Q(\gamma_E) = \frac{Q}{\bar{\chi}_t} - \frac{\chi_n\kappa_c}{\bar{\chi}_t}, \quad (3)$$

$$\Delta\kappa_{\Pi/Q}(\gamma_E) = \frac{\chi_n\kappa_c}{\bar{\chi}_t} \frac{\Pi/Q - Pr_n(B_T/B_P)(\gamma_E/\kappa_c)}{Pr_t(B_T/B_P)(\gamma_E/\kappa_c) - \Pi/Q}. \quad (4)$$

We plot these approximate expressions in Fig. 4(a). The expression for $\Delta\kappa_{\Pi/Q}(\gamma_E)$ is only valid for the transition region between the turbulent and neoclassical regimes, i.e., for $\gamma_{E1} < \gamma_E < \gamma_{E2}$, where γ_{E1} and γ_{E2} are the intersections between the curve $\kappa_c(\gamma_E)$ and the lines (1) and (2), i.e., $Pr_t(B_T/B_P)[\gamma_{E1}/\kappa_c(\gamma_{E1})] = \Pi/Q$ and $Pr_n(B_T/B_P)[\gamma_{E2}/\kappa_c(\gamma_{E2})] = \Pi/Q$. These points of intersection are marked as red squares in Fig. 3(b), and as red dash-dot lines in Fig. 4(a).

The solutions to $Q = Q_b$ and $\Pi/Q = \Pi_b/Q_b$ are given by $\Delta\kappa_Q(\gamma_E) = \Delta\kappa_{\Pi/Q}(\gamma_E)$. In Fig. 4(a), we recast Fig. 3(b) in terms of $\Delta\kappa$. To have several solutions we need type B solutions that we define as intersections where $\Delta\kappa'_Q(\gamma_{E,B}) < \Delta\kappa'_{\Pi/Q}(\gamma_{E,B})$. Here ' denotes differentiation with respect to γ_E . This condition gives

$$\kappa'_c(\gamma_{E,B}) > \frac{1}{Pr_t} \frac{\Pi}{Q} \frac{B_P}{B_T} \left[\frac{\kappa_c(\gamma_{E,B})}{\gamma_{E,B}} \right]^2 \equiv K(\gamma_{E,B}). \quad (5)$$

In Fig. 4(b), the dashed line is κ'_c , and the solid line is $K(\gamma_E)$. Condition (5) is never satisfied near γ_{E1} because $\Delta\kappa'_{\Pi/Q} \rightarrow -\infty$ there.

Condition (5) defines an interval

$$\frac{\Pi}{Q} \Big|_m < \frac{\Pi}{Q} < \frac{\Pi}{Q} \Big|_M \quad (6)$$

outside of which there is only one solution for each Q . Inequality (5) is plotted for $\Pi/Q = \Pi/Q|_m$ and $\Pi/Q = \Pi/Q|_M$ in Figs. 4(c) and 4(d), respectively. At both $\gamma_{E,m}$ and $\gamma_{E,M}$, $\kappa'_c = K$. In addition, $\gamma_{E,m} = \gamma_{E2}$, whereas at

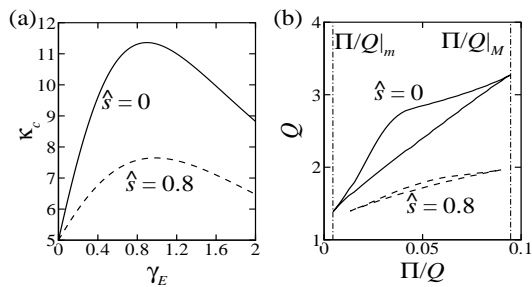


FIG. 5: (a) Critical temperature gradient κ_c for zero (solid line) and finite (dashed line) magnetic shear \hat{s} based on [7] and [6]. (b) Region in the $(\Pi/Q, Q)$ space where abrupt transitions can happen.

$\gamma_{E,M}, \kappa_c'' = K'$. Then, $\gamma_{E,m}$ and $\gamma_{E,M}$ are given by

$$\kappa_c'(\gamma_{E,m}) = \frac{Pr_n \kappa_c(\gamma_{E,m})}{Pr_t \gamma_{E,m}}, \quad (7)$$

$$\kappa_c''(\gamma_{E,M}) = \frac{2\kappa_c'(\gamma_{E,M})}{\gamma_{E,M}} \left[\frac{\gamma_{E,M} \kappa_c'(\gamma_{E,M})}{\kappa_c(\gamma_{E,M})} - 1 \right]. \quad (8)$$

Once $\gamma_{E,m}$ and $\gamma_{E,M}$ are known, $\Pi/Q|_m$ and $\Pi/Q|_M$ can be obtained from $\kappa_c'(\gamma_E) = K(\gamma_E)$, which leads to $\Pi/Q = Pr_t(B_T/B_P)\kappa_c'(\gamma_E)[\gamma_E/\kappa_c(\gamma_E)]^2$. The lower limit $\Pi/Q|_m$ appears because $K(\gamma_E)$ is bounded by its values at γ_{E2} , $(Pr_n^2/Pr_t)(B_T/B_P)(\Pi/Q)^{-1}$, and at γ_{E1} , $Pr_t(B_T/B_P)(\Pi/Q)^{-1}$, tending to infinity for $\Pi/Q \rightarrow 0$. The upper limit $\Pi/Q|_M$ arises because increasing Π/Q shifts the interval $\gamma_{E1} < \gamma_E < \gamma_{E2}$ towards higher values of γ_E and eventually κ_c' becomes negative.

For every Π/Q , there is also an interval in Q ,

$$Q_m < Q < Q_M, \quad (9)$$

for which multiple solutions exist. We show the Q limits for $\Pi/Q = 0.04$ in Fig. 2. The lower limit Q_m is Q_3 and the upper limit Q_M is the meeting point with neoclassical transport.

In Fig. 5(b), we give the domain in the $(\Pi/Q, Q)$ plane where for each Q and Π/Q there are several solutions for κ and γ_E . We do so for zero [7] and finite [6] magnetic shear, whose $\kappa_c(\gamma_E)$ curves are given in Fig. 5(a). The derivative κ_c' is clearly smaller for finite magnetic shear because the velocity shear is less efficient in quenching the turbulence. As a result, as we expect from (5), the region with several solutions is smaller. Thus, transitions are more probable at zero or small magnetic shear.

Conclusions. In tokamaks, the turbulent transport of energy and momentum satisfies two properties: (i) given the energy flux Q , the temperature gradient κ has a maximum possible value achieved at a finite flow shear γ_E ; and (ii) the turbulent Prandtl number Pr_t is approximately constant. Using these properties we have found the optimal level of momentum input. In addition, employing the fact that the neoclassical Prandtl number Pr_n is smaller than Pr_t , we have shown that

transitions to reduced transport can occur in an interval $\Pi/Q|_m < \Pi/Q < \Pi/Q|_M$. Below $\Pi/Q|_m$ the flow shear is not sufficient to suppress the turbulence, and above $\Pi/Q|_M$ the large parallel velocity gradient drives strong turbulence. For each Π/Q , since bifurcations occur only when neoclassical and turbulent transport are comparable and the effective Prandtl number is not constant, Q must be in the interval $Q_m < Q < Q_M$. Below Q_m , the transport is neoclassical or close to neoclassical, and above Q_M , it is mainly turbulent. The region in $(\Pi/Q, Q)$ space where transitions occur is wider for small magnetic shear, which is consistent with both numerical [6, 7] and experimental [2] indications.

The authors are grateful to P. de Vries and G. Hammett for many helpful discussions. This work was supported in part by EPSRC, STFC and the Leverhulme Trust Network for Magnetized Plasma Turbulence.

* Electronic address: f.parradiaz1@physics.ox.ac.uk

- [1] J. W. Connor et al., Nucl. Fusion **44**, R1 (2004).
- [2] P. C. de Vries et al., Nucl. Fusion **49**, 075007 (2009).
- [3] P. C. de Vries et al., Plasma Phys. Control. Fusion **51**, 124050 (2009).
- [4] W. Dorland et al., Plasma Phys. Control. Nucl. Fusion Res. **3**, 463 (1994).
- [5] G. M. Staebler et al., Phys. Plasmas **1**, 909 (1994).
- [6] M. Barnes et al., Phys. Rev. Lett., submitted, arXiv:1007.3390.
- [7] E. G. Highcock et al., Phys. Rev. Lett. **105**, 215003 (2010).
- [8] M. A. Beer et al., Phys. Plasmas **4**, 1792 (1997).
- [9] P. J. Catto, M. N. Rosenbluth and C. S. Liu, Phys. Fluids **16**, 1719 (1973)
- [10] S. L. Newton, S. C. Cowley, and N. F. Loureiro, Plasma Phys. Control. Fusion **52**, 125001 (2010).
- [11] G. R. McKee et al., Nucl. Fusion **49**, 115016 (2009).
- [12] F. L. Hinton and S. K. Wong, Phys. Fluids **28**, 3082 (1985).
- [13] Y. Camenen et al., Phys. Rev. Lett. **102**, 125001 (2009).
- [14] F. I. Parra and P. J. Catto, Plasma Phys. Control. Fusion **52**, 045004 (2010).
- [15] A. G. Peters, C. Angioni and D. Strinzi, Phys. Rev. Lett. **98**, 265003 (2007).
- [16] The simulations in [6, 7] were for an up-down symmetric tokamak and near sonic flow. For large up-down asymmetry [13] or for very subsonic flow [14], Π_t can be driven by temperature and density gradients, and the Prandtl number defined here will not be a constant.
- [17] The effect of a turbulent inward pinch of momentum [15] can be modelled by modifying the momentum input $\Pi = \Pi_b + \text{pinch}$. As a result, $\Pi/Q > \Pi_b/Q_b$.
- [18] Fig. 4(b) of [7] is a numerical reconstruction of Fig. 2.
- [19] For large γ_E , the plasma is linearly stable [7]. Subcritical turbulence exists because small perturbations grow transiently due to temperature and parallel velocity gradients. For turbulence to exist, κ must still be larger than some κ_c .